arXiv:1512.07727v1 [nucl-th] 24 Dec 2015

Investigation of ^{10}Be and its cluster dynamics from nonlocalized clustering concept

Mengjiao Lyu,[1,2,*] Zhongzhou Ren,[1,3,†] Bo Zhou,[4,‡] Yasuro Funaki,[5] Hisashi Horiuchi,[2,6] Gerd Röpke,[7] Peter Schuck,[8,9] Akihiro Tohsaki,[2] Chang Xu,[1] and Taiichi Yamada[10]

[1]*School of Physics and Key Laboratory of Modern Acoustics, Institute of Acoustics, Nanjing University, Nanjing 210093, China*

[2]*Research Center for Nuclear Physics (RCNP), Osaka University, Osaka 567-0047, Japan*

[3]*Center of Theoretical Nuclear Physics, National Laboratory of Heavy-Ion Accelerator, Lanzhou 730000, China*

[4]*Faculty of Science, Hokkaido University, Sapporo 060-0810, Japan*

[5]*Nishina Center for Accelerator-Based Science, The Institute of Physical and Chemical Research (RIKEN), Wako 351-0198, Japan*

[6]*International Institute for Advanced Studies, Kizugawa 619-0225, Japan*

[7]*Institut für Physik, Universität Rostock, D-18051 Rostock, Germany*

[8]*Institut de Physique Nucléaire, Université Paris-Sud, IN2P3-CNRS, UMR 8608, F-91406, Orsay, France*

[9]*Laboratoire de Physique et Modélisation des Milieux Condensés, CNRS-UMR 5493, F-38042 Grenoble Cedex 9, France*

[10]*Laboratory of Physics, Kanto Gakuin University, Yokohama 236-8501, Japan*

(Dated: December 25, 2015)

Abstract

We extend the new concept of nonlocalized clustering to the nucleus ^{10}Be with proton number Z=4 and neutron number N=6 (N=Z+2). The Tohsaki-Horiuchi-Schuck-Röpke (THSR) wave function is formulated for the description of different structures of ^{10}Be. Physical properties such as energy spectrum and root-mean-square radii are calculated for the first two 0^+ states and corresponding rotational bands. With only one single THSR wave function, the calculated results show good agreement with other models and experimental values. We apply, for the first time, the THSR wave function on the chain orbit (σ-orbit) structure in the 0_2^+ state of ^{10}Be. The ring orbit (π-orbit) and σ-orbit structures are further illustrated by calculating the density distribution of the valence neutrons. We also investigate the dynamics of α-clusters and the correlations of two valence neutrons in ^{10}Be.

PACS numbers: 21.60.Gx, 27.20.+n

* mengjiao_lyu@hotmail.com.

† zren@nju.edu.cn.

‡ bo@nucl.sci.hokudai.ac.jp

I. INTRODUCTION

Cluster formation plays a fundamental role in understanding the structure and properties of nuclei. In recent years, tremendous progress has been made in the investigation of cluster structure in light nuclei [1–13], especially due to the model wave function with nonlocalized clustering concept, namely the THSR wave function [1–8]. The THSR wave function was first proposed to describe the α-cluster condensation in gas-like states, including the famous Hoyle state (0_2^+ state) in ^{12}C [1]. Then it was successfully applied to various other aggregates of α-clusters such as ^{8}Be, ^{16}O, ^{20}Ne [1–3], and also to one-dimensional chain systems [5]. It was found that one single THSR wave function is almost 100% equivalent to the RGM/GCM (Resonating Group Method/Generator Coordinate Method) wave functions for both gas-like and non-gaslike states. In the recent studies of inversion-doublet-bands of ^{20}Ne [6, 7], the nonlocalized character of clustering rooted in the THSR wave function is proved to be a very important property for clustering structure in light nuclei. Therefore it is very necessary to investigate the nonlocalized cluster dynamics in other different nuclear systems.

In recent years, there are also investigations using the THSR wave function and its intrinsic container structure for nuclei beyond traditional α aggregates. This starts with the calculation of ^{13}C with a neutron probe interacting with the 3α-condensation [14]. Also, in this year, the 2α+Λ system is investigated with Hyper-THSR wave function, which shows the essential role of the container picture for the cluster structure in $^{9}_{\Lambda}$Be [15]. In our previous work, the THSR wave function is constructed with intrinsic negative parity and applied in the calculation of nucleus ^{9}Be with proton number Z=4 and neutron number N=5 (N=Z+1) [8]. In this study, the nonlocalized clustering concept is shown to prevail in the π-orbit for ^{9}Be.

In order to apply the nonlocalized clustering concept to more general nuclei, it is very interesting to extend the THSR wave function to the investigation of the N=Z+2 cluster nucleus ^{10}Be in which one more valence neutron is added to the ^{9}Be system. The nucleus ^{10}Be is well-known for its typical nuclear molecular orbit structure, and has been studied with many different models [16–23]. The 0_2^+ state of ^{10}Be is considered to be an intruder state which is difficult to be described by simple shell model methods [19]. Besides, a chain structure with σ-binding and enormous spatial extension is found in this 0_2^+ state [17, 18]. Another interesting topic for the N=Z+2 nucleus ^{10}Be is the correlation between valence

neutrons [20]. Recently, predictions of the 0_3^+ and 0_4^+ states [21] and the existence of α+t+t structure in ^{10}Be [22] have been reported. In the present work, we construct THSR wave functions for ^{10}Be based on the new nonlocalized picture. With these THSR wave functions, we can well describe not only the physical properties of different states of ^{10}Be but also the cluster dynamics in these states with only one single THSR wave function.

We organize this paper as follows. In Section II we formulate the THSR wave function for both π- and σ-binding of ^{10}Be. In Section III, we present our results for the 0_1^+ ground state of ^{10}Be and its rotational bands. In Section IV, we investigate the 0_2^+ state of ^{10}Be and its σ-orbit structure. In Section V, we discuss the α-cluster dynamics and correlations between valence neutrons in these states. The last Section VI contains the conclusions.

II. FORMULATION OF THE THSR WAVE FUNCTION FOR ^{10}Be

We first introduce the THSR wave function of ^{10}Be for the π-orbit binding structure of the two valence neutrons without considering their correlations, as shown in the left panel of Fig. 1. This wave function, designated as the independent THSR wave function $|\Phi_{\rm ind}\rangle$, can simply be constructed with the same form as used for ^{9}Be in our previous work [8],

$$\left|\Phi_{\rm ind}(^{10}{\rm Be})\right\rangle = (C_\alpha^\dagger)^2 c_{n,\uparrow}^\dagger c_{n,\downarrow}^\dagger \left|{\rm vac}\right\rangle , \tag{1}$$

where $C_\alpha^\dagger$ and $c_n^\dagger$ are creation operators of α-clusters and valence neutrons, respectively. The α-creator $C_\alpha^\dagger$ determines the dynamics of the α-clusters and can be written as

$$\begin{aligned} C_\alpha^\dagger = \int d^3\mathbf{R} \exp(-\frac{R_x^2}{\beta_{\alpha,xy}^2} - \frac{R_y^2}{\beta_{\alpha,xy}^2} - \frac{R_z^2}{\beta_{\alpha,z}^2}) \int d^3\mathbf{r}_1 \cdots d^3\mathbf{r}_4 \\ \times \psi(\mathbf{r}_1 - \mathbf{R}) a_{\sigma_1,\tau_1}^\dagger(\mathbf{r}_1) \cdots \psi(\mathbf{r}_4 - \mathbf{R}) a_{\sigma_4,\tau_4}^\dagger(\mathbf{r}_4), \end{aligned} \tag{2}$$

where $\mathbf{R}$ is the generate coordinate of the α-cluster, $\mathbf{r}_i$ is the position of the ith nucleon. $a_{\sigma,\tau}^\dagger(\mathbf{r}_i)$ is the creation operator of the ith nucleon with spin σ and isospin τ at position $\mathbf{r}_i$. $\psi(\mathbf{r}) = (\pi b^2)^{-3/4} \exp(-r^2/2b^2)$ is the wave function of a single nucleon in the α-clusters with a Gaussian form where the parameter b in this Gaussian describes the size of α-clusters. $\beta_{\alpha,xy}$ and $\beta_{\alpha,z}$ are parameters for the nonlocalized motion of two α-clusters in horizontal or vertical directions respectively, which is shown as a dashed ellipse in the left panel of Fig. 1. For the valence neutrons, we use the same creation operator $c_n^\dagger$ as in our previous study of

^{9}Be [8]

$$c^\dagger_{n,\sigma} = \int d^3\mathbf{R}_n \exp(-\frac{R^2_{n,x}}{\beta^2_{n,xy}} - \frac{R^2_{n,y}}{\beta^2_{n,xy}} - \frac{R^2_{n,z}}{\beta^2_{n,z}}) e^{im\phi_{\mathbf{R}_n}} \int d^3\mathbf{r}_n \times (\pi b^2)^{-3/4} e^{-\frac{(\mathbf{r}_n - \mathbf{R}_n)^2}{2b^2}} a^\dagger_{\sigma,n}(\mathbf{r}_n), \tag{3}$$

where $\mathbf{R}_n$ is the generate coordinator of the valence neutrons, $\mathbf{r}_n$ is the position of the extra neutron, $a^\dagger_{\sigma,\tau}(\mathbf{r}_n)$ is the creation operator of the extra neutron with spin σ at position $\mathbf{r}_n$, and $\phi_{\mathbf{R}_n}$ is the azimuthal angle in spherical coordinates $(R_{\mathbf{R}_n}, \theta_{\mathbf{R}_n}, \phi_{\mathbf{R}_n})$ of $\mathbf{R}_n$. In this creation operator, the size parameter b of the Gaussian is taken to be the same as that in Eq. (2). $\beta_{n,xy}$ and $\beta_{n,z}$ are parameters for the nonlocalized motion of the extra neutron, shown as solid ellipse in the left panel of Fig. 1.

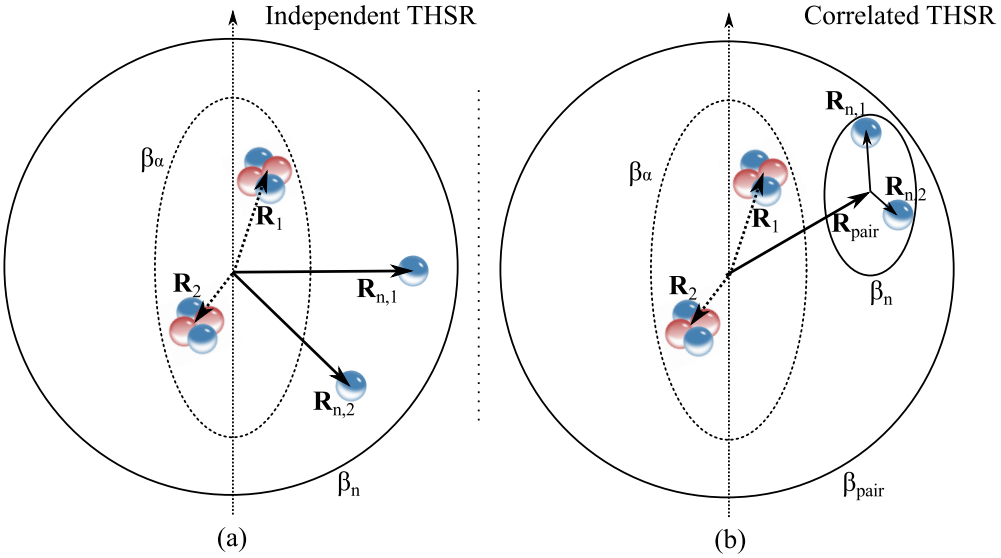

FIG. 1. (Color online.) Generator coordinates and β parameters used in the THSR wave function for the ground state 0^+_1 of ^{10}Be. Left panel (a) shows the case without correlations between valence neutrons. Right panel (b) shows the case of correlated valence neutron motion. Vectors are corresponding generator coordinates. Dashed ellipses denote nonlocalized motion of α-clusters. Solid ellipses denote the nonlocalized motion of the valence neutrons or of the correlated two neutron-valence sub-system.

In Eq. (1), the valence neutrons are assumed to move freely and independently of each other. However, dineutron correlations play an important role for nuclei with two valence nucleons such as ^{6}He and ^{10}Be, as discussed previously in Ref. [20]. The introduction of correlations in the THSR wave function is very natural, because the original THSR wave

function of α-aggregates describes very well the α-α correlations, especially in Refs. [6, 7]. Thus, we can describe the correlation of two valence neutrons in the two-neutron sub-system with a new THSR integration analogously to what we used for two α-clusters.

As shown in the right panel of Fig. 1, two valence neutrons can form a correlated sub-system. The relative position of the valence neutrons in this sub-system is labeled by the generator coordinate $\mathbf{R}_n$, while the position of the correlated sub-system can be described by the generator coordinate $\mathbf{R}_{\rm pair}$. Thus the generator coordinate for the valence neutrons should be $\mathbf{R}_{\rm pair} + \mathbf{R}_n$. With these generator coordinates, we can write the THSR wave function with dineutron correlation in ^{10}Be as

$$\left|\Phi_{\rm cor}(^{10}{\rm Be})\right\rangle = (C_\alpha^\dagger)^2 c_{\rm pair}^\dagger \left|{\rm v}ac\right\rangle, \tag{4}$$

where $c_{\rm pair}^\dagger$ is the creation operator for the dineutron pair, which can be denoted as

$$c_{\rm pair}^\dagger = \int d^3\boldsymbol{R}_{\rm pair} \exp(-\frac{R_{{\rm pair},x}^2}{\beta_{{\rm pair},xy}^2} - \frac{R_{{\rm pair},y}^2}{\beta_{{\rm pair},xy}^2} - \frac{R_{{\rm pair},z}^2}{\beta_{{\rm pair},z}^2}) c_{n,\uparrow}^\dagger(\boldsymbol{R}_{\rm pair}) c_{n,\downarrow}^\dagger(\boldsymbol{R}_{\rm pair}). \tag{5}$$

This integration of $\mathbf{R}_{\rm pair}$ determines the collective motion of the two-neutron sub-system. $\beta_{{\rm pair},xy}$ and $\beta_{{\rm pair},z}$ are parameters for this collective motion, which is shown as the big solid ellipse in the right panel of Fig. 1. $c_{n,\sigma}^\dagger(\boldsymbol{R}_{\rm pair})$ is the creation operator for each neutron, which has a similar form as $c_{n,\sigma}^\dagger$ in Eq. (3),

$$\begin{aligned} c_{n,\sigma}^\dagger(\boldsymbol{R}_{\rm pair}) = & \int d^3\boldsymbol{R}_n \exp(-\frac{R_{n,x}^2}{\beta_{n,xy}^2} - \frac{R_{n,y}^2}{\beta_{n,xy}^2} - \frac{R_{n,z}^2}{\beta_{n,z}^2}) e^{im\phi(\boldsymbol{R}_{\rm pair}+\boldsymbol{R}_n)} \\ & \times \int d^3\boldsymbol{r} (\pi b^2)^{-3/4} e^{-\frac{(\boldsymbol{r}-\boldsymbol{R}_{\rm pair}-\boldsymbol{R}_n)^2}{2b^2}} a_{\sigma,n}^\dagger(\boldsymbol{r}). \end{aligned} \tag{6}$$

This integration of $\mathbf{R}_n$ determines the relative motion of two valence neutrons inside the two-neutron sub-system. $\beta_{n,xy}$ and $\beta_{n,z}$ are parameters for this relative motion, which is shown as small solid ellipse in the right panel of Fig. 1.

As illustrated in Ref. [8], the phase factor $e^{im\phi_{\mathbf{R}_n}}$ in Eq. (3) with parameter $m = \pm 1$ ensures negative parity for the single nucleon wave function of the valence neutron. The same argument can also be applied to the phase factor $e^{im\phi(\boldsymbol{R}_{\rm pair}+\boldsymbol{R}_n)}$ in Eq. (6). Besides, when $m = 0$, only Gaussian functions are left in the creation operators in Eq. (3) or Eq. (6), what corresponds to a positive parity for the valence neutrons. Therefore, we have the total parity of ^{10}Be as

$$\pi = \pi_\alpha^{(1)} \times \pi_\alpha^{(2)} \times \pi_n^{(1)} \times \pi_n^{(2)} = \begin{cases} (+)\times(+)\times(+)\times(+) = + & (m_1 = m_2 = 0) \\ (+)\times(+)\times(-)\times(-) = + & (m_1 = 1, m_2 = -1). \end{cases} \tag{7}$$

For the 0_2^+ state of ^{10}Be, it is already known that this state has a very typical chain structure because of the σ-binding mechanism [17, 24]. In this structure, valence neutrons stay between or outside of two α-clusters along the α-α chain. For this state, we construct the one-dimensional constrained THSR wave function for independent neutrons

$$\left|\Phi_{\rm chain}(^{10}{\rm Be})\right\rangle = (C_\alpha^\dagger)^2 c_{n,\uparrow}^\dagger c_{n,\downarrow}^\dagger \left|{\rm v}ac\right\rangle . \tag{8}$$

Here the α-creation operator $C_\alpha^\dagger$ is similar to Eq. (2) but operates only on the z-axis,

$$\begin{aligned} C_\alpha^\dagger = \int dR_z \exp(-\frac{R_z^2}{\beta_{\alpha,z}^2}) \int d^3\mathbf{r}_1 \cdots d^3\mathbf{r}_4 \\ \times \psi(\mathbf{r}_1 - \mathbf{R}) a_{\sigma_1,\tau_1}^\dagger(\mathbf{r}_1) \cdots \psi(\mathbf{r}_4 - \mathbf{R}) a_{\sigma_4,\tau_4}^\dagger(\mathbf{r}_4), \end{aligned} \tag{9}$$

where $\mathbf{R}$ is the generate coordinate of the α-cluster on the z-axis and $\mathbf{r}_i$ is the position of the ith nucleon. For the valence neutrons, a creation operator with a node structure is constructed for the correct description of the σ-orbits, as

$$\begin{aligned} c_{n,\sigma}^\dagger = \int dR_{n,z}(D - |R_{n,z}|) \exp(-\frac{R_{n,z}^2}{\beta_{n,z}^2}) \int d^3\mathbf{r}_n \\ \times (\pi b^2)^{-3/4} e^{-\frac{(\mathbf{r}_n - \mathbf{R}_n)^2}{2b^2}} a_{\sigma,n}^\dagger(\mathbf{r}_n). \end{aligned} \tag{10}$$

Here, $\mathbf{R}_n$ is the generate coordinate of the valence neutron on the z-axis and $\mathbf{r}_n$ is the position of the valence neutron. We introduce a new factor $(D - |R_{n,z}|)$ in this THSR integration to provide a node structure for the wave function of the valence neutrons. Two nodes appear in the wave function when $R_{n,z} = \pm D$, which are locations near the α-clusters. As a demonstration, we choose parameter $D = 2$ fm and $\beta_{n,z} = 5$ fm, and show the single nucleon wave function $\phi_n(z)$ for valence neutron in Fig. 2. It is clearly seen in the figure that the wave function $\phi_n(z)$ has a different sign between the mid-region and two flanks. Also, two nodes appear near $z = 2$ fm as expected. In our calculation, the parameter D is treated as a variational parameter to obtain a correct node position for the wave function $\phi_n(z)$.

It is obvious that Eq. (9) and Eq. (10) contain only even functions, so the corresponding parity in this wave function is given by,

$$\pi = \pi_\alpha^{(1)} \times \pi_\alpha^{(2)} \times \pi_n^{(1)} \times \pi_n^{(2)} = (+) \times (+) \times (+) \times (+) = +. \tag{11}$$

In order to eliminate effects from spurious center-of-mass (c.o.m.) motion, the c.o.m. part of $|\Phi\rangle$ is projected onto a $(0s)$ state [25]. We use the following transformation of coordinates

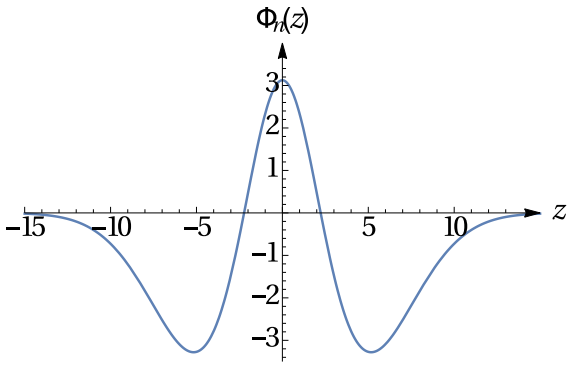

FIG. 2. Single nucleon wave function $\phi_n(z)$ for the valence neutron in the 0_2^+ state of ^{10}Be. Parameters are chosen as $D = 2$ fm and $\beta_{n,z} = 5$ fm.

$\mathbf{r}_i$ in $|\Phi\rangle$ to eliminate the effects of the spurious center-of-mass motion as in Ref. [25]

$$|\Psi\rangle = |(0s)\text{c.o.m.}\rangle\rangle \langle\langle (0s)\text{c.o.m.}|\Phi\rangle \,. \tag{12}$$

Here $(0s)$ represents the wave function of the c.o.m. coordinate $\mathbf{X}_G$ in s-state, and the double brackets denotes the integration with respect to coordinate $\mathbf{X}_G$. We also apply the angular-momentum projection technique $\hat{P}^J_{MK}|\Psi\rangle$ to restore the rotational symmetry [26],

$$\begin{aligned} \left|\Psi^{JM}\right\rangle &= \hat{P}^J_{MK}|\Psi\rangle \\ &= \frac{2J+1}{8\pi^2}\int d\Omega D^{J*}_{MK}(\Omega)\hat{R}(\Omega)|\Psi\rangle \,, \end{aligned} \tag{13}$$

where J is the total angular momentum of ^{10}Be.

The Hamiltonian of the ^{10}Be system can be written as

$$H = \sum_{i=1}^{10} T_i - T_{c.m.} + \sum_{i<j}^{10} V^N_{ij} + \sum_{i<j}^{10} V^C_{ij} + \sum_{i<j}^{10} V^{ls}_{ij}, \tag{14}$$

where $T_{c.m.}$ is the kinetic energy of the center-of-mass motion. Volkov No. 2 [27] is used as the central force of the nucleon-nucleon potential,

$$V^N_{ij} = \{V_1 e^{-\alpha_1 r^2_{ij}} - V_2 e^{-\alpha_2 r^2_{ij}}\}\{W - M\hat{P}_\sigma \hat{P}_\tau \ + B\hat{P}_\sigma - H\hat{P}_\tau\}, \tag{15}$$

where $M = 0.6$, $W = 0.4$ and $B = H = 0.125$. Other parameters are $V_1 = -60.650$ MeV, $V_2 = 61.140$ MeV, $\alpha_1 = 0.309$ fm^{-2}, and $\alpha_2 = 0.980$ fm^{-2}. The G3RS (Gaussian soft core potential with three ranges) term is taken as the two-body type spin-orbit interaction [28],

$$V^{ls}_{ij} = V^{ls}_0\{e^{-\alpha_1 r^2_{ij}} - e^{-\alpha_2 r^2_{ij}}\}\mathbf{L}\cdot\mathbf{S}\hat{P}_{31}, \tag{16}$$

where $\hat{P}_{31}$ projects the two-body system onto triplet odd state. Parameters in V^{ls}_{ij} are taken from Ref. [21] with V^{ls}_0=1600 MeV, α_1=5.00 fm^{-2}, and α_2=2.778 fm^{-2}.

III. THE 0_1^+ GROUND STATE OF ^{10}Be

The Monte Carlo method is used because of its superiority in calculating the numerical integrations in the Hamiltonian kernels, which otherwise is very difficult to be solved analytically for the THSR wave functions of ^{10}Be. The Monte Carlo technique is very flexible for extending the THSR concept. The Monte Carlo calculation includes the integrations of Euler angle Ω in the angular momentum projection and integrations of generate coordinates $\{\mathbf{R}, \mathbf{R}_n\}$ in the creation operators. When using one single THSR wave function, the numerical calculation would be much more efficient than traditional GCM calculations. To compare our results with other models, the width of the Gaussians in the single nucleon wave function is chosen to be $b = 1.46$ fm, which is the same as fixed in Refs. [21, 29]. The β parameters in the THSR wave functions are treated as variational parameters and are optimized with the variational technique.

We investigate the ground state 0_1^+ of ^{10}Be and its rotational band with both the independent THSR wave function and the correlated THSR wave function of ^{10}Be. We choose the parameter $m = 1$ with spin up for one valence neutron and parameter $m = -1$ with spin down for the other. This is to ensure parallel coupling of spin and the orbital angular momentum for both neutrons as we used in previous investigations [8]. The optimum variational parameters for the independent THSR wave function are $\beta_{\alpha,xy} = 0.1$ fm, $\beta_{\alpha,z} = 2.0$ fm, $\beta_{n,xy} = 2.0$ fm and $\beta_{n,z} = 3.5$ fm. For the correlated THSR wave function, the optimum variational parameters are $\beta_{\alpha,xy} = 0.1$ fm, $\beta_{\alpha,z} = 2.2$ fm, $\beta_{\mathrm{pair},xy} = 0.8$ fm, $\beta_{\mathrm{pair},z} = 1.8$ fm, $\beta_{n,xy} = 2.0$ fm and $\beta_{n,z} = 2.7$ fm.

In Table I, we list the calculated results of the 0^+ ground state of ^{10}Be together with results from other models and experimental values. The binding energies obtained for the ground state 0_1^+ are -58.0 MeV and -58.2 MeV with independent and correlated THSR wave functions, respectively. Theoretical calculations with other models, in which the same potential is used, provide binding energies of the ground state of ^{10}Be ranging from about -59 MeV to -60 MeV, which is about 1$\sim$2 MeV lower than our results [20, 29]. This difference is reasonable because we are using only one single THSR wave function what may not be the optimal choice for the valence neutrons. If we superpose 8 THSR wave functions with different parameters β for α-clusters or valence neutrons in the THSR wave function, the ground state energy would decrease to -59.0 MeV, which is consistent with

other methods, as shown in Table I. The experimental value for the ground state of ^{10}Be is -65.0 MeV, which is much lower than any theoretical results from our and other groups' works. These differences originate from the choice of effective potentials.

From these results, we can also notice that the binding energy of the ground state is improved by about 0.2 MeV by the introduction of the valence neutron correlation in the THSR wave function. This improvement shows the correlation effect of the valence neutrons in the ground state, as we will discuss later in Section V.

In our present calculation, the ansatz of Gaussians (multiplied by factors) is used for the valence neutron in the THSR wave functions. In the future, we will discuss more general form of the THSR wave function for a better optimized description of the valence neutrons.

TABLE I. Results obtained for the 0^+ ground state of ^{10}Be. $\mathrm{THSR_{ind}}$ and $\mathrm{THSR_{cor}}$ are binding energies calculated with the independent THSR wave function and the correlated THSR wave function, respectively. $\mathrm{THSR_{\Sigma 8}}$ denotes calculated result by superposing 8 different THSR wave functions. Results from other theoretical methods are also listed.

Model	E (MeV)
$\mathrm{THSR_{ind}}$	-58.0
$\mathrm{THSR_{cor}}$	-58.2
$\mathrm{THSR_{\Sigma 8}}$	-59.0
AMD[20]	-58.7
AMD+DC[20]	-60.4
AMD+GCM[29]	-59.2

We show in Fig. 3 the energy spectrum of the 0_1^+ rotational band of ^{10}Be based on the ground state. The calculated excitation energy of the 2_1^+ state is 3.5 MeV and fits very well with the experimental value 3.4 MeV. Good agreement can also be seen between our calculation and the AMD method for the 2_1^+ and 4_1^+ excited states.

The root-mean-square radius of the 0_1^+ ground state of ^{10}Be is also obtained from our approach. The result is 2.57 fm with one single THSR wave function, which is consistent with the value 2.5 fm from Ref. [21], but slightly larger than the value 2.37 fm from Ref. [20] and the experimental value 2.30 fm. This small difference originates from the slightly weaker

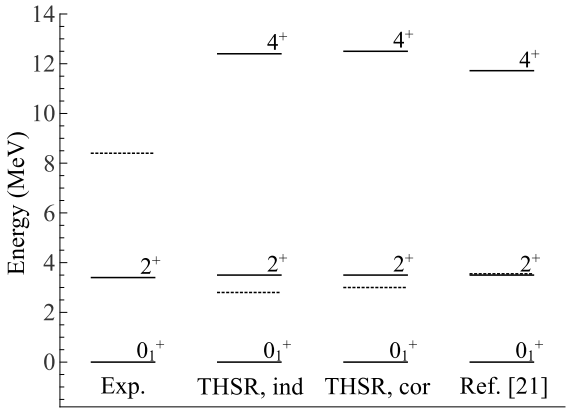

FIG. 3. The 0^+ ground state of ^{10}Be and its rotational band. "THSR,ind" and "THSR,cor" denote calculated results with the independent THSR wave function and the correlated THSR wave function, respectively. "Ref. [21]" denotes the results of the AMD method [21]. "Exp." denotes the experimental result. The dashed lines indicate the corresponding $\alpha + \alpha + n + n$ threshold -55.2 MeV.

binding effect described by only one single THSR wave function, as discussed above.

The density distribution $\rho(\mathbf{r}'_n)$ of the extra nucleons is calculated to give a clear view of the dynamics of the valence neutrons. The intrinsic wave function $|\Psi\rangle$ of ^{10}Be can be written in the following form

$$|\Psi\rangle = \mathrm{C}\mathcal{A}[\Phi^{\mathrm{THSR}}(2\alpha)\phi_{\mathrm{pair}}(\mathbf{r}_1, \mathbf{r}_2)], \tag{17}$$

where $\mathcal{A}$ is the antisymmetrizer and C is a normalization constant. Then the density distribution $\rho(\mathbf{r}')$ of the valence neutrons is defined as

$$\rho(\mathbf{r}') = N_c\langle\Phi^{\mathrm{THSR}}(2\alpha)\phi_{\mathrm{pair}}(\mathbf{r}_1, \mathbf{r}_2)|\delta(\mathbf{r}_1 - \mathbf{X}_G - \mathbf{r}') + \delta(\mathbf{r}_2 - \mathbf{X}_G - \mathbf{r}')|\Psi\rangle, \tag{18}$$

where N_c is the normalization constant [30]. As shown in Fig. 4, the density distribution of two valence neutrons has the same shape as the one which we obtained for the ground state ^{9}Be [8] with only a single valence neutron. The extension of the density distribution in the z-direction and the absence of neutrons along the z-axis shows a good description of the π-orbit in the ground state of ^{10}Be as suggested by nuclear molecular orbit (MO) model [16, 17]. This reproduction of π-orbit structure is obtained naturally from the antisymmetrization in the THSR wave function which cancels non-physical distribution of valence neutrons, e.g. positions close to the center of α-clusters.

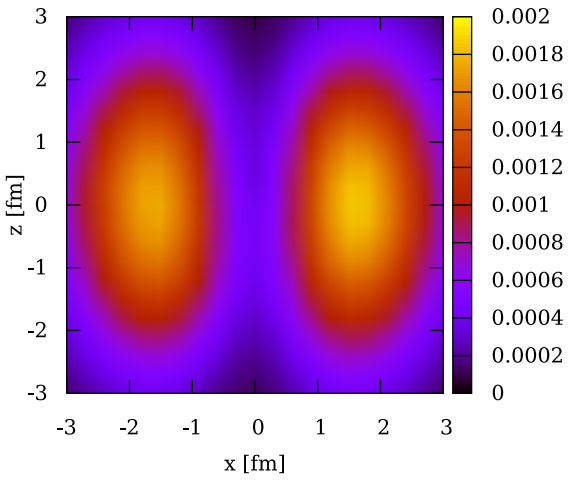

FIG. 4. (Color online.) Density distribution of the valence neutrons in the intrinsic ground state of ^{10}Be. The color scale of each point in the figure is proportional to the nucleon density on $x-z$ plane of the $y=0$ cross section. The unit of the density is fm^{-3}.

IV. THE 0_2^+ CHAIN STATE OF ^{10}Be

In this section we study the 0_2^+ state of ^{10}Be with one single THSR wave function as shown in Eq. (8). The optimum parameter D in Eq. (10) is $D = 2.0$ fm. Other optimum variational parameters in the THSR wave function are $\beta_\alpha = 3.5$ fm and $\beta_n = 4.0$ fm. The calculated spectrum for the 0_2^+ rotational band based on the ground state is shown in Fig. 5. The ground state energy from THSR calculation in this figure is chosen to be the one with -59.0 MeV obtained from the superposed THSR wave functions as listed in Table I. Fig. 5 shows systematical discrepancies between theoretical results calculated by different models and the experimental values. This is because of the choice of effective interactions. The calculated energy spectrum of the 0_2^+ rotational band with the THSR wave function, as shown in Fig. 5, agrees well with results of other theoretical models from Refs. [21, 29]. The THSR wave function also gives energy gaps between the states in the 0_2^+ band which fit very well with experimental data and other models. It is very interesting to see that one single THSR wave function can describe well the 0_2^+ state of ^{10}Be, while in other theoretical models superposition of large number of basis sets is needed.

We checked the orthogonality between the THSR wave function for the 0_2^+ state and the 0_1^+ ground state. The calculated overlap between these two states is 1.4%, which satisfies the requirement for eigenstates.

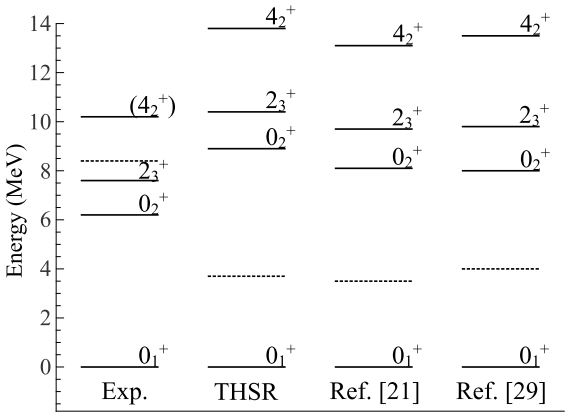

FIG. 5. Energy spectrum of the 0_2^+ rotational band relative to the ground state energy. The one labeled with Ref. [21] is the value calculated with the AMD+DC method [21]. The one labeled with Ref. [29] is the value calculated with the $\beta-\gamma$ constrained AMD+GCM method [29]. The dashed lines are the corresponding $\alpha+\alpha+n+n$ thresholds of -55.2 MeV.

We also calculate the root-mean-square radius for the 0_2^+ state of ^{10}Be. The calculated result is 3.11 fm, which is consistent with 2.96 fm from Ref. [20] and 3.4 fm from Ref. [21].

To illustrate the structure of the 0_2^+ state of ^{10}Be with the THSR wave function, we show the density distribution $\rho(\mathbf{r}'_n)$ of valence nucleons in Fig. 6. It is clearly seen that the distribution of valence neutrons is divided into three regions separated by two nodes perpendicular to the z-axis, which is a typical character of the σ-orbit. The node structure originates from the newly introduced factor $(D-|R_{n,z}|)$ in Eq. (10). Also a large spread of more than 10 fm along the z-axis is observed for the valence neutrons, which is one of the reasons for the enormously large spatial extension of the 0_2^+ state in ^{10}Be. Another reason is the large α-cluster distribution as discussed in the next section.

V. ANALYSIS OF CLUSTER DYNAMICS AND DINEUTRON CORRELATIONS

In this section, we discuss the dynamics of the α-clusters and the valence neutrons. The THSR wave function is based on the nonlocalized concept of cluster dynamics which describes the α-cluster motion by a Gaussian style THSR integration of generator coordinates as in Eq. (2) or Eq. (9). The optimum β-parameters in the α-creation operators is $\beta_{\alpha,xy}\approx 0$ fm, $\beta_{\alpha,z}=2.0$ fm for the ground 0_1^+ state while the optimum value $\beta_\alpha=3.5$ fm is obtained for the 0_2^+ state. Considering that large β parameters corresponds to large extension of the

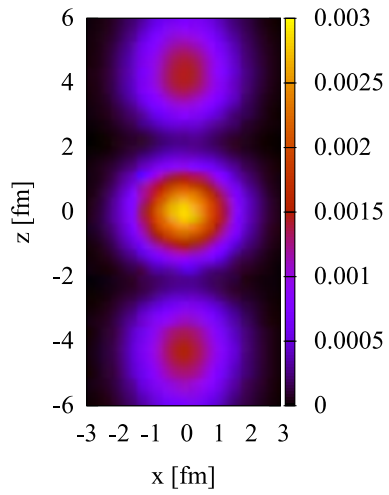

FIG. 6. (Color online.) Density distribution of valence neutrons in the intrinsic 0_2^+ state of ^{10}Be. The color scale of each point in the figure is proportional to the nucleon density in the $x-z$ plane of the $y=0$ cross section. The unit of the density is fm^{-3}.

nonlocalized cluster motion, it is clear that the α-particles are much more tightly bound by the $\pi-$orbit than by the σ-orbit. The π-binding effect in the ground state of ^{10}Be is also stronger than that in the ground state of ^{9}Be, where the optimum parameter for α-cluster is $\beta_{\alpha,z} = 4.2$ fm [8].

Another interesting problem is the dineutron correlation effect in the ^{10}Be nucleus. With the correlated THSR wave function, we calculate the contour map of the binding energy surface for the ground state of ^{10}Be as shown in Fig. 7. For simplicity, we fix the deformation between x, y and z directions to be 0. The optimum binding energy locates near the coordinates $(1.5, 2.0)$, where $\beta_{\text{pair},xy} = \beta_{\text{pair},z} = 1.5$ fm and $\beta_{n,xy} = \beta_{n,z} = 2.0$ fm. This optimum value is slightly higher than the final result of -58.2 MeV because deformation is neglected here. When $\beta_{\text{pair}} = 0$, the center of the two-neutron sub-system is fixed at the origin of coordinates, and the correlated THSR wave function turns to become an independent one for the two neutrons. Thus, the optimum value of parameter $\beta_n > 0$ shows the existence of correlation effects in the ground state, as discussed above. Large distance between the two neutrons in the dineutron pair can be concluded because of the big value of the parameter β_n. The relatively small value of the parameter β_{pair} describes the collective motion of the two-neutron sub-system. We also study the correlation of the two valence neutrons in the 0_2^+ state of ^{10}Be. A very large value of the parameter β_n is obtained which shows nearly

independent motion of the two valence neutrons in this state.

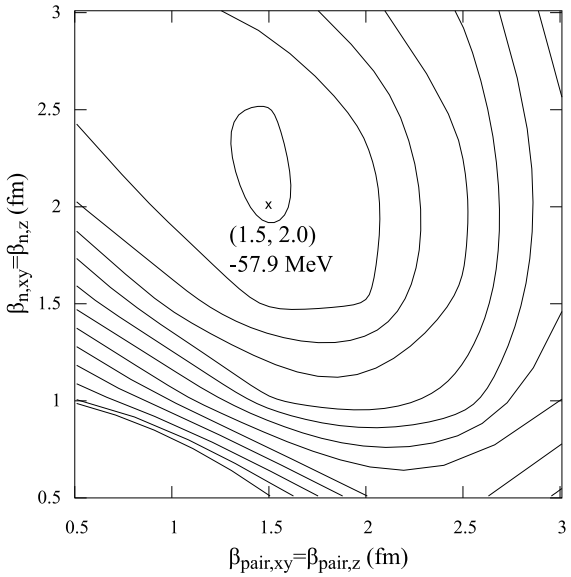

FIG. 7. Contour map of the binding energy surface of the ground state with different β parameters in the correlated THSR wave function. The horizontal coordinates are the $\beta_{\rm pair}$ parameters for the center-of-mass of two valence neutrons as $\beta_{{\rm pair},xy} = \beta_{{\rm pair},z}$. The vertical coordinates are the β_n parameters for each neutron in the two neutron sub-system as $\beta_{n,xy} = \beta_{n,z}$. Other parameters are $\beta_{\alpha,xy} = 0.1$ fm,$\beta_{\alpha,z} = 2.0$ fm. The optimum value is marked on the map labeled with corresponding coordinates.

VI. CONCLUSION

We investigated the N=Z+2 nucleus ^{10}Be from the nonlocalized clustering concept. THSR wave functions with π-orbit structure and chain (σ-orbit) structure are formulated for ^{10}Be. Correct parity and node structures are ensured in THSR wave functions for the corresponding states. The 0^+_1 ground state of ^{10}Be and its rotational band is calculated and the results agree well with other models and experimental values. Small improvement is observed for the binding energy of the ground state with introduction of correlations between two valence neutrons in a single one THSR wave function. The 0^+_2 state is also studied with the newly formulated THSR wave function containing a node factor. The calculated energy spectrum of the 0^+_2 rotational band is consistent with values from other models as well as with experiments. This result is very interesting because only one single THSR wave function is used.

Root-mean-square radii are also calculated for the first two 0^+ states of ^{10}Be, which have good agreements with other models. The density distribution of valence neutrons shows good description of σ-orbit by the THSR wave function. It is the first application of the nonlocalized picture to σ-orbit binding systems. Analysis of optimum β parameters shows much tighter binding effect for α-clusters within the π-orbit structure than with the σ-orbit structure. Showing the contour map of energy calculated with correlated THSR wave function, we discussed the correlation effect between valence neutrons and also the intrinsic and collective motion of the di-neutron pair in the ground state. The investigation of ^{10}Be is another extension of the nonlocalized concept and of the THSR wave function towards more general nuclear structures. Our calculations with the THSR wave function and the Monte Carlo technique requires less numerical work than the traditional GCM treatment. Also, the THSR wave function used in this work illustrates more physical insights of the ^{10}Be nucleus. In the future, this scheme based on nonlocalized concept is also promising for the study of neutron-rich nuclei with cluster structures and the investigations of their corresponding cluster and nucleon dynamics.

ACKNOWLEDGMENTS

The authors would like to thank Professor Kanada-En'yo-san for valuable discussions. This work is supported by the National Natural Science Foundation of China (grant nos 11535004, 11375086, 11120101005, 11175085 and 11235001, 11575082), by the 973 National Major State Basic Research and Development of China, grant nos 2013CB834400 and by the Science and Technology Development Fund of Macao under grant no. 068/2011/A.

[1] A. Tohsaki, H. Horiuchi, P. Schuck, and G. Röpke, Phys. Rev. Lett. **87**, 192501 (2001).

[2] Y. Funaki, H. Horiuchi, A. Tohsaki, P. Schuck, and G. Röpke, Prog. Theor. Phys. **108**, 297 (2002).

[3] Bo Zhou, Zhongzhou Ren, Chang Xu, Yasuro Funaki, Taiichi Yamada, Akihiro Tohsaki, Hisashi Horiuchi, Peter Schuck, and Gerd Röpke, Phys. Rev. C **86**, 014301 (2012).

[4] T. Yamada and P. Schuck, Eur. Phys. J. A **26**, 185 (2005).

[5] T. Suhara, Y. Funaki, B. Zhou, H. Horiuchi, and A. Tohsaki, Phys. Rev. Lett. **112**, 062501 (2014).

[6] Bo Zhou, Yasuro Funaki, Hisashi Horiuchi, Zhongzhou Ren, Gerd Röpke, Peter Schuck, Akihiro Tohsaki, Chang Xu, and Taiichi Yamada, Phys. Rev. Lett. **110**, 262501 (2013).

[7] Bo Zhou, Yasuro Funaki, Hisashi Horiuchi, Zhongzhou Ren, Gerd Röpke, Peter Schuck, Akihiro Tohsaki, Chang Xu, and Taiichi Yamada, Phys. Rev. C **89**, 034319 (2014).

[8] Mengjiao Lyu, Zhongzhou Ren, Bo Zhou, Yasuro Funaki, Hisashi Horiuchi, Gerd Röpke, Peter Schuck, Akihiro Tohsaki, Chang Xu, and Taiichi Yamada, Phys. Rev. C **91**, 014313 (2015).

[9] Y. Kanada-En'yo, H. Horiuchi, and A. Ono, Phys. Rev. C **52**, 628 (1995).

[10] Chang Xu and Zhongzhou Ren, Phys. Rev. C **73**, 041301 (2006).

[11] Yuejiao Ren and Zhongzhou Ren, Phys. Rev. C **85**, 044608 (2012).

[12] Wanbing He, Yugang Ma, et al., Phys. Rev. Lett. **113**, 032506 (2014).

[13] Zaihong Yang, Yanlin Ye, et al., Phys. Rev. Lett. **112**, 162501 (2014).

[14] A. Tohsaki, Int. J. Mod. Phys. E **17**, 2106 (2008).

[15] Y. Funaki, T. Yamada, E. Hiyama, B. Zhou, and K. Ikeda, Prog. Theor. Exp. Phys. 113D01 (2014).

[16] W. von Oertzen, Z. Phys. A **354**, 37 (1996).

[17] N. Itagaki and S. Okabe, Phys. Rev. C **61**, 044306 (2000).

[18] M. Ito, K. Kato, and K. Ikeda, Phys. Lett. B **588**, 43 (2004).

[19] E. K. Warburton, B.A. Brown, Phys. Rev. C **46**, 923 (1992).

[20] F. Kobayashi and Y. Kanada-Enyo, Prog. Theor. Phys. **126**, 457 (2011).

[21] F. Kobayashi and Y. Kanada-Enyo, Phys. Rev. C **86**, 064303 (2012).

[22] N. Itagaki, M. Ito, M. Milin, T. Hashimoto, H. Ishiyama, and H. Miyatake, Phys. Rev. C **77**, 067301 (2008).

[23] T. Myo, A. Umeya, H. Toki, and K. Ikeda, Prog. Theor. Exp. Phys. 63D03 (2015).

[24] Y. Ogawa, K. Arai, Y. Suzuki, and K. Varga, Nucl. Phys. A **673**, 122 (2000).

[25] S. Okabe, Y. Abe, and H. Tanaka, Prog. Theor. Phys. **57**, 866 (1977).

[26] P. Ring and P. Schuck, *The Nuclear Many-Body Problem* (Springer-Verlag, New York, 1980), p. 474.

[27] A. B. Volkov, Nucl. Phys. **74**, 33 (1965).

[28] N. Yamaguchi, T. Kasahara, S. Nagata, and Y. Akaishi, Prog. Theor. Phys. **62**, 1018 (1979).

[29] T. Suhara and Y. Kanada-Enyo, Prog. Theor. Phys. **123**, 303 (2010).

[30] H. Horiuchi, Prog. Theor. Phys. Supple. **62**, 90 (1977).